

# Temperature driven changes of the graphene edge structure on Ni(111): substrate vs. hydrogen passivation

*Laerte L. Patera,<sup>1,2</sup> Federico Bianchini,<sup>1,†</sup> Giulia Troiano,<sup>3</sup> Carlo Dri,<sup>1,2</sup> Cinzia Cepek,<sup>2</sup> Maria Peressi,<sup>1,4,5,\*</sup>*

*Cristina Africh,<sup>2,\*</sup> Giovanni Comelli<sup>1,2,3,6</sup>*

<sup>1</sup> Department of Physics, Università degli Studi di Trieste, via Alfonso Valerio 2, 34127 Trieste, Italy

<sup>2</sup> IOM-CNR Laboratorio TASC, Area Science Park, s.s. 14 km 163.5, Basovizza, 34149 Trieste, Italy

<sup>3</sup> Elettra – Sincrotrone Trieste S.C.p.A. , s.s. 14 km 163.5, Basovizza, 34149 Trieste, Italy

<sup>4</sup> IOM-CNR DEMOCRITOS National Simulation Center Trieste, Italy

<sup>5</sup> Consorzio Interuniversitario Nazionale per la Scienza e la Tecnologia dei Materiali (INSTM), Unità di ricerca di Trieste, piazzale Europa 1, 34128 Trieste, Italy

<sup>6</sup> Center of Excellence for Nanostructured Materials (CENMAT), Università degli Studi di Trieste, via Alfonso Valerio 2, 34127 Trieste, Italy

## Possible edge structures

As explained in the main text, the edge configurations that are in best agreement with the experimental images are  $z/z_1$  and  $k/rk_1$  at  $470^\circ\text{C}/\text{RT}$ , respectively. In **Figure S11** we show the simulated STM images of these structures obtained both doing a conventional cut of the energy-integrated local density of states (ILDOS) at a constant height from the surface (central part of each panel) and mapping an ILDOS iso-surface (left part). The best agreement with the experimental images reported in Figure 2 of the paper is obtained by using the conventional cut at a constant height from the surface for  $z$  and  $k$  edges (experimental images detected in the quasi-constant height mode by FAST STM scan), and mapping an ILDOS iso-surface for  $z_1$  and  $rk_1$  edges (experimental images detected in the constant-current STM measurements post-growth).

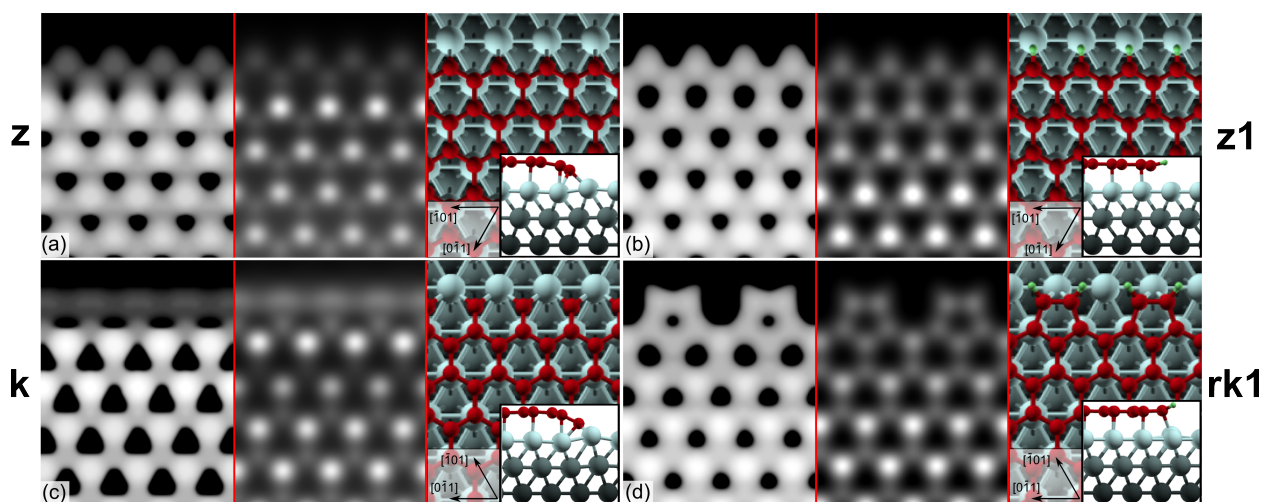


**Figure S11** Atomic structure of  $z$ ,  $z_1$ ,  $k$  and  $rk_1$  graphene edges on Ni(111) and simulated DFT STM images obtained doing a conventional cutting of the energy-integrated local density of states (ILDOS) at a constant height from the surface (central part of each panel) and mapping an ILDOS iso-surface (left part).

The main structural difference between hydrogenated/clean edges is the bending toward the substrate of the latter. This feature is clearly present in both experimental and simulated images, as shown in **Figure S12** for  $z/z_1$  edges. In the case of the  $z_1$  edge, the profiles of the constant-current STM images experimentally detected and the DFT-simulated images with the

mapping of an ILDOS iso-surface are not in perfect agreement, but it is difficult to identify the best matching between the parameters of the experimental scan and the simulated ILDOS isovalue. Furthermore, corrugation in the experimental line profile of z1 is reduced due to limited imaging resolution.

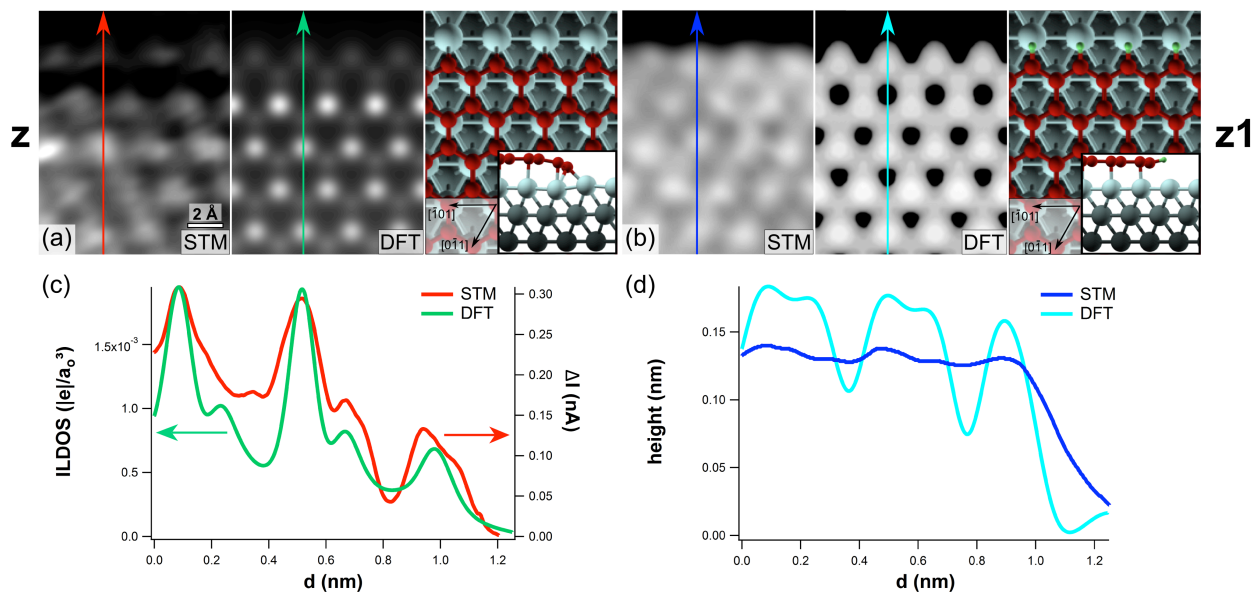


**Figure S12:** Atomic structure and experimental STM and DFT-simulated images for z (a) and z1 (b) graphene edges on Ni(111). Panel (c): profiles of the current intensity in the experimental STM scan and of the DFT-calculated energy-integrated local density of states (ILDOS) for the z edge, along the lines indicated in (a). Panel (d): Height profiles of the constant current STM image and of an isosurface of the DFT-calculated ILDOS for the z1 edge, along the lines indicated in (b).

In addition to the edge configurations presented above, other structures have been tested. The rk configuration (**Figure S13**) is stable, but can be excluded for the non-hydrogenated edges both on the basis of the comparison between experimental and simulated STM images (there is no evidence of double periodicity in the experimental images), and because of energetics (the total energy is 0.3 eV per each terminal C atom at the edge higher than the corresponding system with k edge; details in the Thermodynamics section).

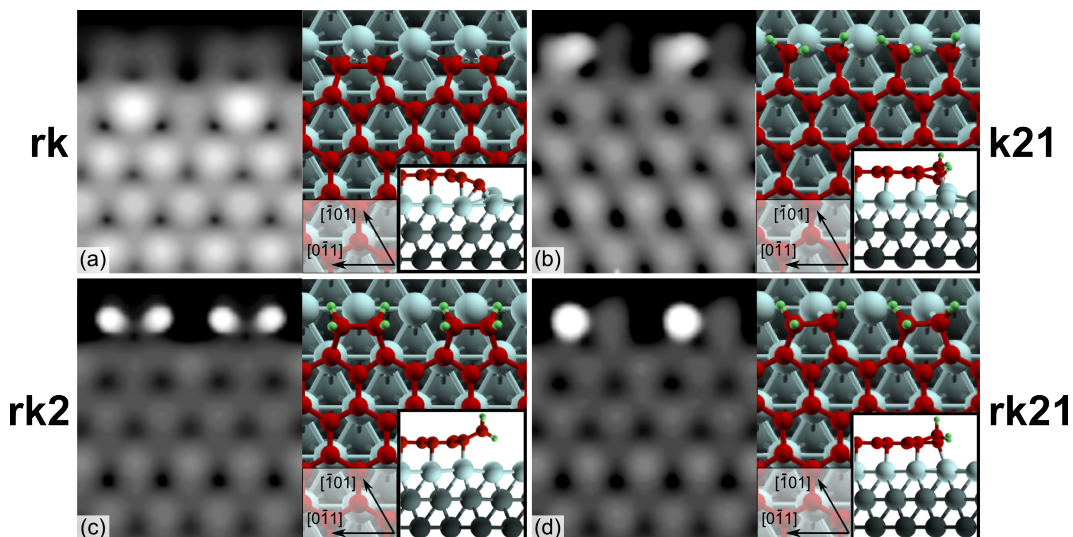


**Figure S13:** DFT-simulated images and stick-and-ball models of the calculated geometries for different stable non-hydrogenated and hydrogenated configurations not included in the main text. The images for hydrogenated configurations are obtained in constant current mode with an energy-integrated density of states isovalue of  $7 \times 10^{-5} |e|/a_0^3$ ; the image for the non-hydrogenated configuration is obtained in constant height mode at a distance of 0.5 Å from graphene.

**Figure S13** also shows the stick-and-ball model and the calculated STM image of hydrogenated stable structures with more than one hydrogen atom for each terminal C atom. We label each structure with the number of H atoms attached to the edge C atoms, using a single number if all such C atoms are equivalent, or two numbers if two adjacent terminal C atoms bring a different number of H atoms. Therefore, k21 and rk21 indicate edges with adjacent terminal C atoms di- and mono-hydrogenated respectively, and rk2 indicates the edge characterized by structure rk with *each* terminal C atom di-hydrogenated. The energy gain for the second hydrogenation of the reconstructed Klein edges, defined as the difference in total energy of the considered system with respect to rk1 (the other edge of the ribbon being z1 in both cases) and molecular hydrogen in gas phase, is much lower than the first hydrogenation energies. The energy gain for the second hydrogenation for rk21 and rk2 is respectively 0.02 eV and 0.33 eV per carbon atom at the edge. The k21 configuration is very unfavored with respect to rk21, being the total energy of the former higher than the latter by 0.49 eV per edge terminal C atom. However, a barrier prevents the edge reconstruction and makes the k21 configuration stable.

All these stable structures with more than one hydrogen for each terminal C atom (rk2, k21, and rk21) can be excluded because there are no experimental STM images showing the strong asymmetry in the edges or the difference in height with respect to the other part of the ribbon appearing in the simulated images.

Other hydrogenated edges are not stable and, upon optimization of the structure, evolve toward other stable configurations: k1 into rk1, and k2 into rk2.

Zig-zag edges with more than one hydrogen atom for each terminal C atom, as z12 or z2, do not exist: excess hydrogen atoms can combine each other, forming desorbing H<sub>2</sub> molecules, as occurs starting from z2, or bind to the surface, as found in some simulation where the starting z12 tends to transform into z1.

## Hydrogenation

Concerning hydrogenation, it could involve a large number of different paths, whose precise identification is beyond the scope of the present paper. As an example, we report the energy diagram of one of them, referring to the z edge, in **Figure SI4**: i) an H<sub>2</sub> molecule approaches a clean Ni patch on the surface, where it dissociatively adsorbs with an exothermic process giving 0.57 eV for H atom; ii) each H atom requires about 0.5 eV to reach the terminal edge C atom, where the formation of the C-H bond lifts the edge breaking the C-Ni bond. We stress that along this hydrogenation path the energy of the system remains always below its initial value, indicating that the overall hydrogenation process is practically barrierless, apart from a possible negligible barrier for the dissociative adsorption of the H<sub>2</sub> molecule on the Ni surface (extensively characterized in the wide existing literature cited in the main text).

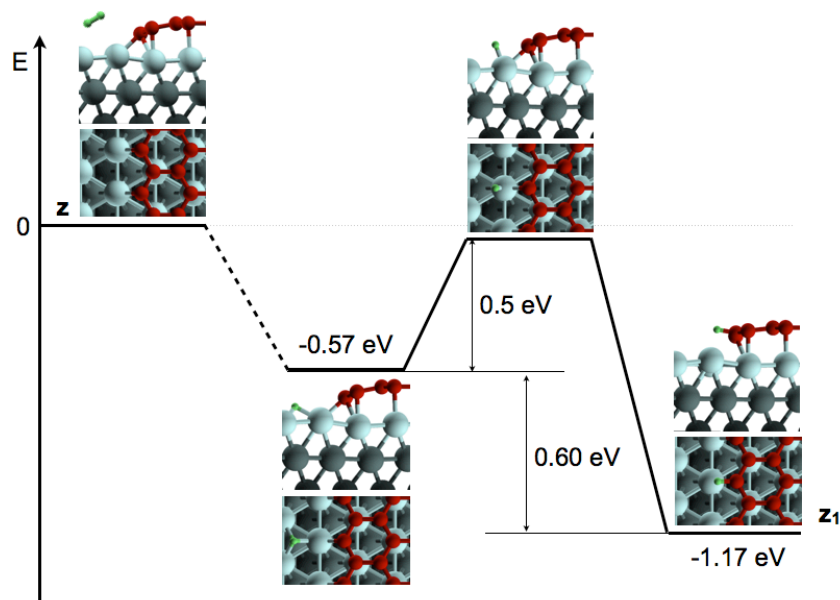


**Figure SI4:** DFT energy diagram of a particular path for the hydrogenation of z edges. The zero of the energy corresponds to the surface passivated z edge and to the H<sub>2</sub> molecule in gas phase. Energies are referred to each terminal C atom .

## Thermodynamics

A complete overview of the thermodynamics of the different possible edge structures, calculated by DFT at 0K allows us to finalize the picture of the formation of the edges and further corroborates our findings. As a consequence of the lack of inversion symmetry of the substrate, a direct estimate of the individual *edge adsorption energy* is not accessible, since the nanoribbon geometry used to simulate the flakes necessarily shows different edges *in pairs*, like the opposite sides of the hexagonal island shown in Figure 1c. It is therefore straightforward to consider *pairs* of different edges, combining z and k structures, and calculate their average adsorption energy. This can be done by subtracting the total energies of the free-standing graphene nanoribbon and of the substrate to the total energy of the system (graphene adsorbed on Ni), and further reducing it by the contribution to the adsorption of the C atoms not pertaining to the edges, which is -0.16 eV/atom for epitaxial graphene in top-fcc configuration<sup>1</sup>. We show in **Figure S15** the results for the *edge adsorption energy* per pairs of non-hydrogenated z and k edges and hydrogenated z1 and rk1 edges. As expected, the z-k pair of non-hydrogenated edges, corresponding to the strong covalent bond with the substrate, has the largest adsorption energy, estimated to be -3.92 eV/pair of terminal C atoms, with respect to other pairs of edges, and the z1-rk1 pair the smallest, -0.85 eV/pair of C atoms. Intermediate and similar values are found for pairs of edges including one hydrogenated and one not hydrogenated terminations, z-rk1 and z1-k, with adsorption energies equal to -2.33 and -2.53 eV/pair of C atoms respectively. For the sake of completeness, we also mention the adsorption energies for the edge pairs containing rk, although not observed in real samples, namely -2.24 and -3.63 eV/pair of terminal C atoms for z1-rk and z-rk respectively. Considering all these values, we can conclude that the edge contribution to the adsorption of a flake is always relevant with respect to the inner part, also in absence of passivation of the substrate, but the anchoring to the metal through a covalent bond gives an additional energy gain of about 1.5 eV per each terminal C atom. We also observe, comparing z1-rk with z1-k and z-rk with z-k, that rk is 0.30 eV/ terminal C atom less favored than k.

A similar value is obtained if we compare the energy gain upon edges hydrogenation for free standing and supported graphene: the difference between 2.65 (2.67) eV/terminal C atom for z (rk) edges, respectively, and 1.17 (1.09) eV for z (k) edges respectively is also about 1.5 eV and must be attributed to the absence/presence of the covalent bond of the edge with the substrate.

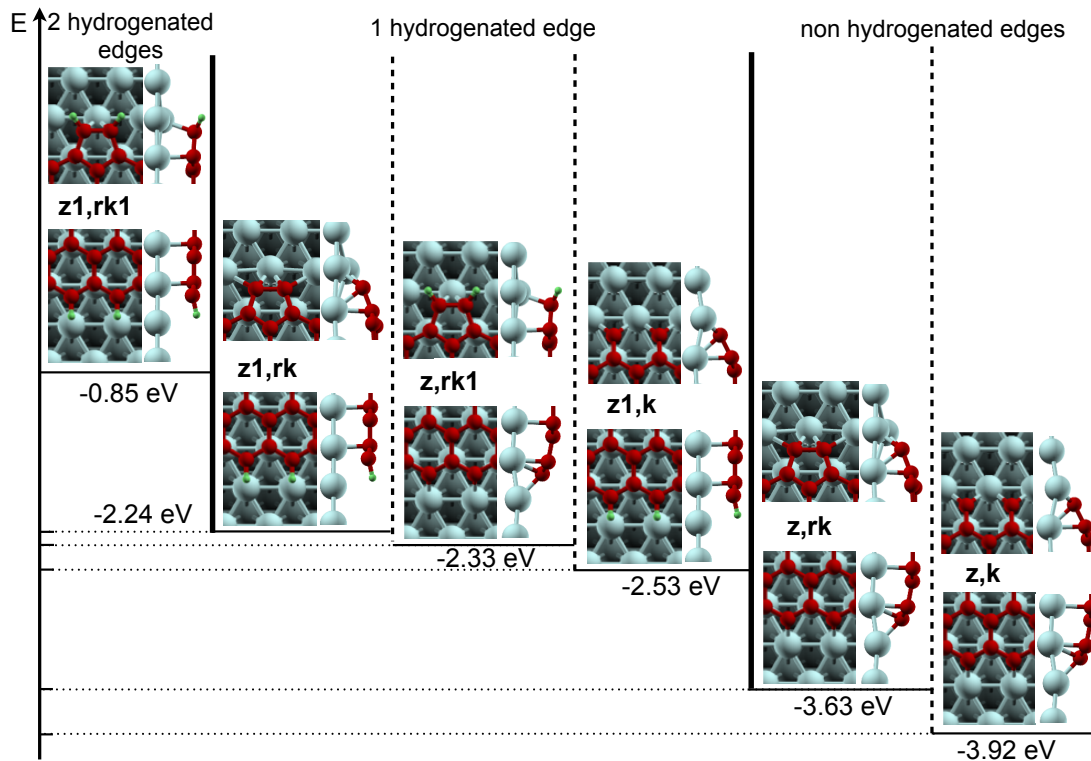


**Figure S15:** DFT adsorption energy diagram of *edge pairs* of graphene on Ni(111). The energies are given per pair of terminal C atoms of the edges.

### Convergence of energetics, structural and electronic properties with the ribbons width

The adsorption energy per terminal C atoms in a pair of edges can be obtained also with a different procedure. We have calculated the average adsorption energy, inclusive of edges contribution, for ribbons of different width: since the adsorption is stronger at the edges than in the internal regions, the average adsorption energy decreases in intensity with increasing the width of the ribbon. This is shown in **Figure S16** for ribbons with z-k edges, referred to free-standing ribbons with the same pair of edges, but the behavior for ribbons with other terminations is similar. A fit of these data with a function taking into account the contributions of the C atoms at the edges and those in the internal region of the ribbon gives an estimate of the two contributions. We obtain -0.15 eV for each internal C atom, in excellent agreement with the value of -0.16 eV mentioned above for an infinite epitaxial graphene. Concerning the edge contribution, we obtain -5.48 eV per pair of C atoms at the edges, to be compared with the value of -5.36 eV obtained from the largest ribbon after subtraction of the contribution of -0.16 eV for each internal C atom (the value of -3.92 in Figure S13 is referred to the lowest energy free-standing ribbon configuration which is z-rk and not z-k).

Figure SI4 indicates how delicate the convergence of the energetics with the ribbon width is, and justifies our use of very large ribbons (41 rows of C atoms). The electronic properties are also quite sensitive to the ribbon width: a ribbon with 41 rows of C atoms is necessary to have the STM imaging of the central part of the ribbon resembling the one of the infinite graphene layer. Conversely, the structural properties are much less sensitive to the ribbon width: a ribbon with only 11 rows of C atoms (the smallest considered in Figure SI6) is flat in the central part, where its distance from the Ni surface already recovers the one characterizing an infinite graphene layer (2.1 Å).

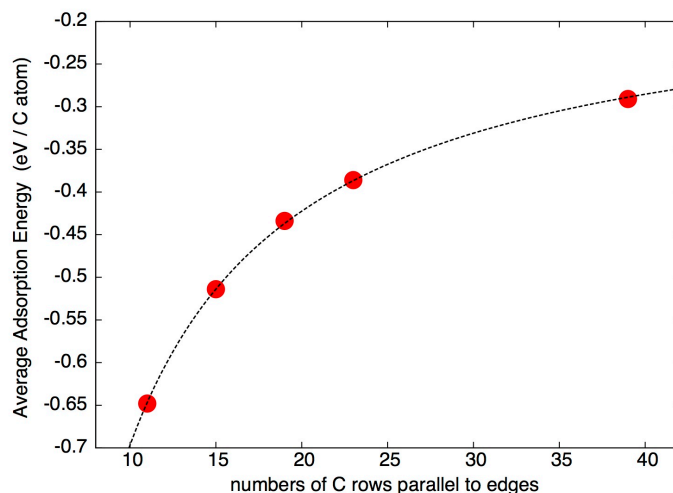


**Figure SI6:** DFT average adsorption energy (eV/ C atom) for graphene ribbons on Ni(111) terminated with the pair of z-k edges as a function of the width of the ribbons, expressed in terms of number of zig-zag C atom rows parallel to the edges.

## REFERENCE

- (1) Bianchini, F.; Patera, L. L.; Peressi, M.; Africh, C.; Comelli, G. *J. Phys. Chem. Lett.* **2014**, *5*, 467–473.